Experimental and Theoretical Studies of the Kinetics of the Reactions of OH Radicals with Acetic Acid, Acetic Acid-d_3 and Acetic Acid-d_4 at Low Pressure

Deepali Vimal and Philip S. Stevens*

Institute for Research in Environmental Science, School of Public and Environmental Affairs, and Department of Chemistry, Indiana University, Bloomington, Indiana 47405

Received: May 25, 2006; In Final Form: August 3, 2006

The kinetics of the reactions of OH with acetic acid, acetic acid-d_3 and acetic acid-d_4 were studied from 2 to 5 Torr and 263−373 K using a discharge flow system with resonance fluorescence detection of the OH radical. The measured rate constants at 300 K for the reaction of OH with acetic acid and acetic acid-d_4 ($CD_3C(O)OD$) were $(7.42 \pm 0.12) \times 10^{-13}$ and $(1.09 \pm 0.18) \times 10^{-13}$ cm^3 molecule^{-1} s^{-1} respectively, and the rate constant for the reaction of OH with acetic acid-d_3 ($CD_3C(O)OH$) was $(7.79 \pm 0.16) \times 10^{-13}$ cm^3 molecule^{-1} s^{-1}. These results suggest that the primary mechanism for this reaction involves abstraction of the acidic hydrogen. Theoretical calculations of the kinetic isotope effect as a function of temperature are in good agreement with the experimental measurements using a mechanism involving the abstraction of the acidic hydrogen through a hydrogen-bonded complex. The rate constants for the OH + acetic acid and OH + acetic acid-d_4 reactions display a negative temperature dependence described by the Arrhenius equations $k_H(T) = (2.52 \pm 1.22) \times 10^{-14} \exp((1010 \pm 150)/T)$ and $k_D(T) = (4.62 \pm 1.33) \times 10^{-16} \exp((1640 \pm 160)/T)$ cm^3 molecule^{-1} s^{-1} for acetic acid and acetic acid-d_4, respectively, consistent with recent measurements that suggest that the lifetime of acetic acid at the low temperatures of the upper troposphere is shorter than previously believed.

Introduction

Acetic acid is an abundant oxygenated volatile organic compound present in the troposphere with mixing ratios of approximately 1−2 ppbv.[1−3] Acetic acid is an important contributor to the acidity of precipitation and cloudwater and is also important in determining the rates of pH-dependent chemical transformations.[4−8] Concentrations of acetic acid in the atmosphere are subject to both seasonal and diurnal variations, suggesting both biogenic and photochemical sources.[4,6,9,10] Direct biogenic sources include soil and vegetation emissions, and direct anthropogenic emissions include biomass burning and motor vehicle exhaust.[4,6,9−18] Secondary atmospheric photochemical sources of acetic acid include reactions of peroxyacetyl radicals, formed by the oxidation of acetaldehyde and the photolysis of acetone, with HO_2 and CH_3O_2.[19−25] These secondary photochemical reactions are considered to be the predominant source of acetic acid, accounting for about 120 Tg yr^{-1} and making up about 70% of the global production,[26] with biomass burning contributing approximately 48 Tg yr^{-1} to the global source strength of acetic acid.[11] Several studies have pointed out the possible existence of unknown photochemical sources that might contribute to the high concentrations of acetic acid observed in the upper troposphere.[18,27,28]

Dry and wet deposition are the predominant removal processes for acetic acid due to its limited chemical transformation, as it reacts comparatively slowly with the hydroxyl radical (OH).[4,6,9,10,17,29] The reaction of acetic acid with OH is thought to dominate if heterogeneous removal processes are inefficient, especially in the upper troposphere and lower stratosphere:[26,30,31]

$$CH_3C(O)OH + OH \rightarrow CH_3C(O)O + H_2O \rightarrow CH_3 + CO_2 + H_2O \quad (1a)$$

$$\rightarrow CH_2C(O)OH + H_2O \quad (1b)$$

The reaction between OH and acetic acid has been the subject of several kinetic studies.[30,32−34] Zetzsch and Stuhl used flash-photolysis coupled with resonance fluorescence detection of OH and obtained a rate constant $k_1 = (5.99 \pm 0.78) \times 10^{-13}$ cm^3 molecule^{-1} s^{-1} at 298 K and between 20 and 500 Torr.[32] The temperature dependence of the rate constant for reaction 1 was investigated by Dagaut et al. between 240 and 440 K and 25−50 Torr using flash-photolysis coupled with resonance fluorescence detection of OH, reporting a positive temperature-dependent rate of $k_1(T) = ((1.3 \pm 0.1) \times 10^{-12}) \exp(-(170 \pm 20)/T)$ cm^3 molecule^{-1} s^{-1}, and a value of $(7.4 \pm 0.6) \times 10^{-13}$ cm^3 molecule^{-1} s^{-1} at 298 K.[33] In contrast, Singleton et al., using laser flash photolysis coupled with resonance absorption detection of OH, found a negative temperature dependence over the temperature range 297−445 K and 500 Torr with a rate constant $k_1(T) = (7.79 \times 10^{-14}) \exp(679/T)$ cm^3 molecule^{-1} s^{-1} and a value of 7.6×10^{-13} cm^3 molecule^{-1} s^{-1} at 297 K.[34]

These results have led to a recommended value of $k_1(T) = (4 \times 10^{-13}) \exp(200 \pm 400/T)$ cm^3 molecule^{-1} s^{-1} with a rate constant of 8×10^{-13} cm^3 molecule^{-1} s^{-1} at 298 K.[35] However, Butkovskaya et al. have recently reported results from a high-pressure turbulent flow study at 200 Torr over the temperature range 229−300 K using a chemical ionization mass spectrometer for detection of OH.[30] They observed a stronger negative

* Corresponding author. E-mail address: pstevens@indiana.edu.

10.1021/jp063224y CCC: $33.50
Published on Web 09/21/2006

temperature dependence for the reaction, obtaining a rate constant expression of $k_1(T) = ((2.2 \pm 0.2) \times 10^{-14}) \exp((1012 \pm 80)/T)$ cm^3 molecule^{-1} s^{-1} and a value of $(6.6 \pm 0.8) \times 10^{-13}$ cm^3 molecule^{-1} s^{-1} at 298 K.[30] Combining their results between 229 and 300 K with the earlier results of Singleton et al. between 297 and 445 K,[34] Butkovskaya et al. obtained a three-parameter expression describing the temperature dependence of this reaction:[30]

$$k_1(T) = (2.45 \times 10^{-16})(T/298)^{5.24} \pm 0.68 \exp((2358 \pm 189)/T) \text{ cm}^3 \text{ molecule}^{-1} \text{ s}^{-1} \quad (2)$$

They concluded from the above expression that the reaction proceeds with a rate constant of 2.2×10^{-12} cm^3 molecule^{-1} s^{-1} at 220 K, which is greater than the recommendation of Sander et al.[35] This is an important result for the chemistry of the upper troposphere, where average temperatures are in the range 220−240 K. Butkovskaya et al. have estimated a residence time for acetic acid of 9.4 days in the upper troposphere on the basis of the faster rate constant and an average OH concentration of 5.5×10^5 molecules cm^{-3}. They concluded that this reaction might be an efficient source of methyl peroxy radicals and a net source of HO_x radicals in the upper troposphere.[30]

As a result of the published discrepancies in the measurements of the rate constant for the reaction of OH with acetic acid as a function of temperature, further kinetic and mechanistic studies are required to accurately assess the role of acetic acid in atmospheric chemistry. This paper examines the low pressure (2−5 Torr) kinetics of the rate constant of the reaction of OH radicals with acetic acid and its deuterated isotopomers, acetic acid-d_3 ($CD_3C(O)OH$) and acetic acid-d_4 ($CD_3C(O)OD$), between 263 and 373 K. These are the first measurements of the temperature dependence and the kinetic isotope effect for this reaction at pressures less than 20 Torr. Theoretical calculations are also used to determine if the observed kinetic isotope effect is consistent with a mechanism for this reaction involving hydrogen abstraction through the formation of an intermediate complex.

Experimental Methods

Experiments were performed using the discharge-flow technique with resonance fluorescence detection of the OH radicals. Detailed descriptions of the experimental technique have been given elsewhere.[36−39] The reactor consists of a jacketed 1 m long, 2.54 cm diameter Pyrex glass tube which has ports to allow the addition of gases. A movable injector (0.3 cm o.d.) inserted in the middle of the reactor is used for the introduction of acetic acid. Both the tube and the injector were coated with Halocarbon wax (Halocarbon Corporation) to minimize the loss of radicals on these surfaces. Average flow velocities of approximately 10 m s^{-1} were maintained by using a Leybold D16B mechanical pump downstream of the radical detection zone. The reaction temperature was varied by circulating heated silicone oil or liquid nitrogen cooled ethanol through the jacket of the flow-tube, and the temperature was monitored using a thermocouple located in the center of the reaction zone. Bulk flows of helium were regulated using a MKS 1179 flow meter to maintain total pressure of approximately 2−5 Torr, measured by a MKS Baratron capacitance manometer.

OH radicals were produced by the fast reaction of H radicals with NO_2:

$$H + NO_2 \rightarrow OH + NO \quad (k^{II} = 1.3 \times 10^{-10} \text{ cm}^3 \text{ molecule}^{-1} \text{ s}^{-1}) \quad (3)$$

H atoms were produced from a microwave discharge (Opthos Instruments) of H_2 in He. NO_2 concentrations of approximately 6×10^{13} molecules cm^{-3} were added in excess 2 cm upstream of the radical source to ensure rapid conversion of H atoms to OH.

OH radicals were detected by resonance fluorescence using the $A^2\Sigma(v=0)\Sigma \rightarrow X^2\Pi(v=0)$ transition near 308 nm. The light source was a lamp consisting of a flowing He/H_2O mixture excited using microwave radiation. A photomultiplier tube (Hamamatsu H6180-01) equipped with photon counting electronics at a right angle to the radiation source was used to detect the OH fluorescence, and darkened baffles and light traps fitted on the opposite side of the detector were used to reduce background scatter in the chamber. An interference filter centered at 308 nm (Esco Products) with a 10 nm band-pass and a transmission of 20% was used to isolate the OH fluorescence. The system sensitivity was approximately 1×10^{-8} counts s^{-1} cm^3 molecule^{-1} on the basis of calibrations using reaction 3 and resulted in a minimum detectable limit of approximately 1×10^9 molecules cm^{-3} for OH (background signal = 300−400 counts s^{-1}, S/N = 1, 10 s integration). Initial OH concentrations of less than 3×10^{11} molecules cm^{-3} were used for all of the experiments.

Heterogeneous loss of OH onto the reactor walls was observed with addition of acetic acid to the reactor at low temperatures, as the observed pseudo-first-order decays of OH were nonlinear, leading to large positive intercepts in the second-order plots. The loss is thought to occur when OH undergoes heterogeneous reactions with acetic acid adsorbed to the walls of the reactor. This behavior has previously been observed in the OH + acetone,[39] isoprene,[36,37] the Cl + isoprene,[40,41] and the OH + α-, β-pinene reactions.[42,43] The addition of oxygen (approximately $(2-5) \times 10^{15}$ cm^{-3}) minimized the acetic acid-catalyzed loss of OH radicals on the wall of the reactor, resulting in linear and reproducible first-order decays and intercepts in the second-order plots of less than 10 s^{-1} without affecting the measurements of the second-order rate constants. The addition of oxygen appears to reduce the acetic acid-catalyzed loss of OH by inhibiting active wall sites.[39] Measurements above room temperature were done both with and without oxygen, whereas oxygen was added for measurements below room temperature.

Acetic acid was purified by trap-to-trap distillation with the middle fraction retained and the top and bottom fractions rejected; the distillation was performed by pumping until the acetic acid volume was reduced to 20−50%, followed by several freeze−pump−thaw cycles. Mixtures containing 0.5−3% acetic acid were prepared by vacuum distilling the purified acetic acid into a 5.5 L calibrated reservoir fitted with a capacitance manometer and diluting the mixture with helium to a pressure of about 760 Torr. At the partial pressures of the acetic acid used to make these mixtures, the majority (greater than 80%) of the acetic acid present was in its dimer form:

$$2CH_3C(O)OH \leftrightarrows (CH_3C(O)OH)_2 \quad (4)$$

However, on the basis of the equilibrium constant for the dimerization, these dimers dissociated at the low pressure in the flow tube, and this was taken into consideration when the concentrations of acetic acid were calculated. The dimerization equilibrium constant is given by

$$K_{eq} = P_D/P_M{}^2 = (7.1 \times 10^{-9}) \exp(7705/T) \text{ atm}^{-1} \quad (5)$$

where P_D and P_M are dimer and monomer partial pressures given in atmospheres.[44−46] Acetic acid ($(1.2-20.0) \times 10^{13}$ molecule

TABLE 1: Summary of Experimental Results

T (K)	10^{-13}[acetic acid] (molecules cm^{-3})	rate constant (10^{-13} cm^3 molecule^{-1} s^{-1})	pressure (Torr)	no. of exp
		OH + acetic acid		
273	1.8−10.3	9.09 ± 0.12	5	16
300	1.2−20.0	7.42 ± 0.12	2−5	82
323	2.2−12.1	4.92± 0.31	5	32
353	4.6−16.6	4.39 ± 0.28	5	25
373	1.0−20.0	4.1 ± 0.77	5	15
		OH + acetic acid-d_4		
263	2.5−24.9	2.34 ± 0.29	5	14
273	1.5−24.3	1.9 ± 0.24	5	16
300	1.1−29.8	1.09 ± 0.18	5	32
323	1.4−32.8	0.70 ± 0.24	5	12
		OD + acetone-d_3		
300	1.1−19.1	7.79 ± 0.16	5	35

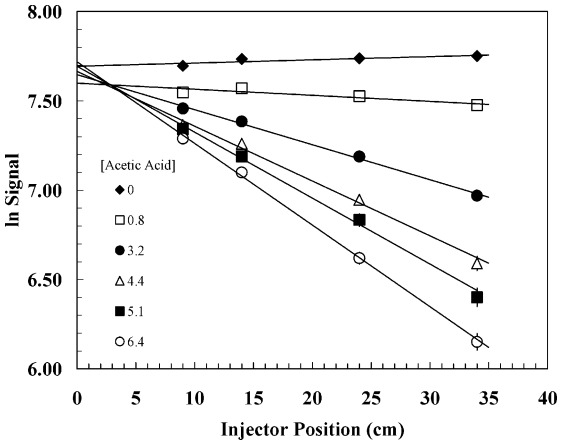

Figure 1. First-order plot for the OH + acetic acid reaction at 300 K and 5 Torr. Acetic acid concentrations are in units of 10^{13} molecules cm^{-3}. Error bars represent 2σ uncertainty and are generally smaller than the size of the points.

cm^{-3}) was introduced into the flow tube through the movable injector, and concentrations were determined by measuring the pressure drop in the calibrated reservoir over time. To correct for the loss of OH radicals onto the surface of the movable injector, an experiment was performed without the addition of acetic acid, resulting in a reproducible increase in the OH signal as the injector is pulled out. This small increase in the observed signal is due to the decrease in the surface area exposed to OH radicals as the injector is pulled out of the reactor.

The following gases and chemicals were used in these experiments: NO_2 (1.1% in He, Mathseon), H_2 (Ultrahigh Purity 99.999%, Indiana Oxygen), zero-grade He (99.995%, Indiana Oxygen), acetic acid (>80% acid by mass, Mallinckrodt Chemicals), and acetic acid-d_3 and -d_4 (Sigma Aldrich, 99 atom % D).

Results

A summary of the experimental conditions is listed in Table 1. Experiments were conducted at 5 Torr with additional measurements conducted at 2 Torr. All experiments were conducted under pseudo-first-order conditions. Figure 1 shows an example of typical pseudo-first-order decays of OH at various concentrations of acetic acid. Pseudo-first-order decay rates (k^I) were calculated from a weighted linear least-squares fit (based on the signal-to-noise ratio of each measurement) of the logarithm of the OH fluorescence signal versus reaction time, as determined from the reaction distance under the plug-flow approximation (k^I_{decay}), and values of k^I were corrected for axial diffusion and OH loss on the movable injector as follows:[47]

$$k^I = k^I_{decay}\left(1 + k^I_{decay}\frac{D}{v^2}\right) - k_{injector} \qquad (6)$$

Here D is the diffusion coefficient for OH in He ($0.145T^{2/3}P$ in Torr cm^2 s^{-1}), v is the average bulk gas flow velocity (8.9−13.6 m s^{-1}) and $k_{injector}$ is the rate of loss of OH on the injector measured in absence of acetic acid (<10 s^{-1}).

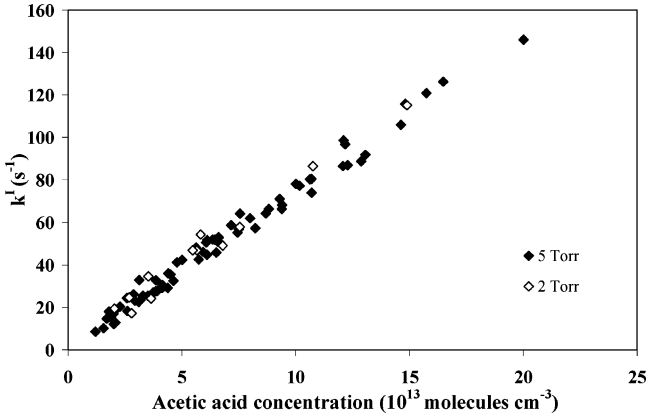

Figure 2. Second-order plots for the OH + acetic acid reaction at 300 K and 2 and 5 Torr.

OH + Acetic Acid. Figure 2 shows the second-order plot for the OH + acetic acid reaction at 300 K and pressures of 2 and 5 Torr. The experiments at 5 Torr and 300 K for the OH + acetic acid reaction were repeated in the presence of water (approximately 10^{16} molecules cm^{-3}) with no observed effect on the measured rate constant. From these experiments the second-order rate constant for the OH + acetic acid reaction at 300 K was determined to be (7.42 ± 0.12) × 10^{-13} cm^3 molecule^{-1} s^{-1}, independent of pressure between 2 and 5 Torr. The error is twice the standard deviation from the weighted fit of the rate constant data on the basis of the precision of each measurement.[48] This value is in good agreement with the recommended rate constant of 8 × 10^{-13} cm^3 molecule^{-1} s^{-1},[35] and the previous studies by Zetzsch and Stuhl between 22 and 500 Torr (k_1 = (5.99 ± 0.78) × 10^{-13} cm^3 molecule^{-1} s^{-1} at 298 K),[32] Dagaut et al. between 25 and 50 Torr (k_1 = (7.4 ± 0.6) × 10^{-13} cm^3 molecule^{-1} s^{-1} at 298 K),[33] Singleton et al. at 500 Torr (k_1 = (8.6 ± 0.6) × 10^{-13} cm^3 molecule^{-1} s^{-1}),[34] and Butkovskaya et al. at 200 Torr (k_1 = (6.6 ± 0.8) × 10^{-13} cm^3 molecule^{-1} s^{-1} at 298 K).[30]

A plot of the measured rate constants versus inverse temperature for the OH + acetic acid reaction is shown as the upper set of data in Figure 3. A weighed fit of the rate constants measured in this study as a function of inverse temperature results in the following Arrhenius expression: (2.52 ±1.22) × 10^{-14} exp((1010 ± 150)/T) cm^3 molecule^{-1} s^{-1} (upper dashed line in Figure 3), in excellent agreement with the Arrhenius expression obtained by Butkovskaya et al.,[30] corresponding to a negative activation energy of approximately 2 kcal mol^{-1}.

Figure 3 also compares the results of this study with previous measurements and recommendations for the rate constant for this reaction as a function of temperature. The upper solid line in Figure 3 represents the rate constant for the OH + acetic acid reaction calculated using the three parameter expression given by Butkovskaya et al.[30] (eq 2), and the dash−dot line is the recommendation of Sander et al.[35] As can be seen from this figure, the low-pressure measurements of the rate constant for

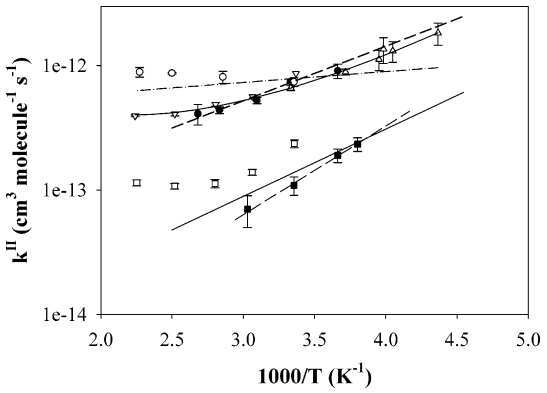

Figure 3. Arrhenius plot for the OH + acetic acid and the OH + acetic acid-d_4 reactions. The upper symbols represent data for the OH + acetic acid reaction: this work (●); Dagaut et al.[33] (○); Singleton et al.[34] (▽); Butkovskaya et al.[30] (△). The dashed line is a weighted Arrhenius fit of the data in this study, and the solid line represents the three-parameter expression recommended by Butkovskaya et al.[30] The dash−dot line is the recommendation of Sander et al.[35] The lower symbols represent data for the OH + acetic acid-d_4 reaction: this work (■), Singleton et al.[34] (□). The dashed line is a weighted Arrhenius fit of the data in this study, and the solid line represents the calculated rate constant for the OH + acetic acid-d_4 reaction based on the abstraction of the acidic hydrogen through a pre-reactive complex (see text).

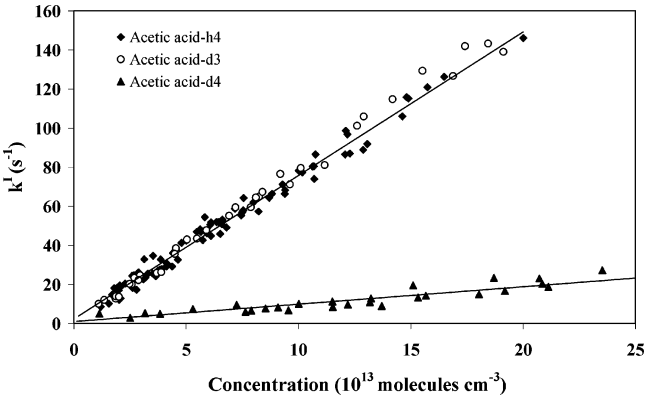

Figure 4. Second-order plots for the OH + acetic acid, OH + acetic acid-d_3, and the OH + acetic acid-d_4 reactions at 300 K and 5 Torr.

the OH + acetic acid reaction between 263 and 373 K reported here are in excellent agreement with the previous studies at higher pressures between 296 and 446 K by Singleton et al.,[34] and between 229 and 300 K by Butkovskaya et al.[30] In addition, the rate constants reported here are in good agreement with their three-parameter expression that describes the curvature above 298 K observed by Singleton et al.,[34] although we were unable to observe any significant curvature over the temperature range of this study. The results presented here are in contrast to the positive temperature dependence observed by Dagaut et al.[33] One possible reason for the discrepancy in the results of Dagaut et al. may be heterogeneous loss of acetic acid on the walls of the reactor and the assumption that the rates of reaction of OH with acetic acid monomer and dimer were equal at low temperatures.[34] Unfortunately, increased heterogeneous effects in this study prevented measurements of the rate constant at temperatures below 263 K. Additional experimental measurements, especially at temperatures above 400 K and below 250 K, are needed to further confirm the temperature dependence for this reaction.

OH + Acetic Acid-d_3 and OH + Acetic Acid-d_4. Figure 4 shows the second-order plot for the OH + acetic acid-d_3 reaction at 300 K and 5 Torr. A weighted fit of these data results in a rate constant of $(7.79 \pm 0.16) \times 10^{-13}$ cm^3 molecule^{-1} s^{-1}. This value is in excellent agreement with the rate constant of $(8.1 \pm 0.22) \times 10^{-13}$ cm^3 obtained by Singleton et al. at 297 K and 500 Torr[34] and is similar to the rate constant of the OH + acetic acid reaction (k_1). This suggests that the primary mechanism for the reaction involves abstraction of the acidic hydrogen rather than hydrogen abstraction from the methyl group. Figure 4 also shows the second-order plot for the OH + acetic acid-d_4 reaction at 300 K and 5 Torr, resulting in a rate constant of $(1.09 \pm 0.18) \times 10^{-13}$ cm^3 molecule^{-1} s^{-1}. This result is lower than the value of $(2.35 \pm 0.17) \times 10^{-13}$ cm^3 molecule^{-1} s^{-1} obtained by Singleton et al. at 297 K and 500 Torr.[34] The reason for this discrepancy is unclear. One possible explanation may be uncertainties associated with the high concentrations of acetic acid required to observe significant OH decays in our experiments.

A plot of the measured rate constants versus inverse temperature for the OH + acetic acid-d_4 is also shown in Figure 3, and a weighted fit of the data yields an Arrhenius expression of $k = (4.62 \pm 1.33) \times 10^{-16} \exp((1640 \pm 160)/T)$ cm^3 molecule^{-1} s^{-1} between 273 and 323 K, resulting in a negative activation energy of approximately 3.3 kcal mol^{-1} (lower dashed line in Figure 3). The temperature dependent rate constants measured in this study are generally lower than those measured by Singleton et al.,[34] although the negative activation energies are similar over the temperature range of this study. As with the OH + acetic acid reaction, we did not observe any significant curvature in the Arrhenius plot for the OH + acetic acid-d_4 reaction. Unfortunately, measurements of the rate constant at temperatures higher than 323 K were unsuccessful due to the inability to introduce concentrations of acetic acid-d_4 high enough to generate reproducible OH decays.

Discussion

The reaction between OH and acetic acid is thought to proceed either by carboxylic hydrogen abstraction (1a) or by direct abstraction of a methyl hydrogen (1b).[30,34,49] Recent measurements of a CO_2 yield of (64 ± 17)% for the reaction between 249 and 300 K using chemical ionization mass spectrometry suggests that reaction 1a is the predominant pathway,[30] consistent with the measurements of the kinetic isotope effect for both the OH + acetic acid-d_3 and OH + acetic acid-d_4 reported here and by Singleton et al.[34] Recently, De Smedt et al. also measured the CO_2 yield from reaction 1a to be (64 ± 14)% using mass-spectrometry at 290 K and 2 Torr.[50]

The abstraction occurring preferentially at the acidic hydrogen is unexpected because the strength of the C−H bond is smaller than that of O−H bond (bond dissociation energies of (98.3 ± 1.8) and (105.8 ± 2) kcal mol^{-1}, respectively). This anomalous result can be explained by the formation of a hydrogen-bonded pre-reactive complex that lowers the energy of the acidic hydrogen abstraction pathway.[30,34,49,50] Recent ab initio calculations of the potential energy surface for the OH + acetic acid reaction suggest that the reaction should proceed primarily through abstraction of the acidic hydrogen via several hydrogen-bonded pre-reactive complexes, with the complex for the acidic-H abstraction channel more stable than that for the methyl-H abstraction channel.[50,51] Addition of OH to the central carbonyl carbon and abstraction of the methyl hydrogen were found to have activation energies that were significantly larger than abstraction of the acidic hydrogen, with the barrier to OH addition large enough to make this channel insignificant under atmospheric conditions.[50,51] This mechanism is similar to that

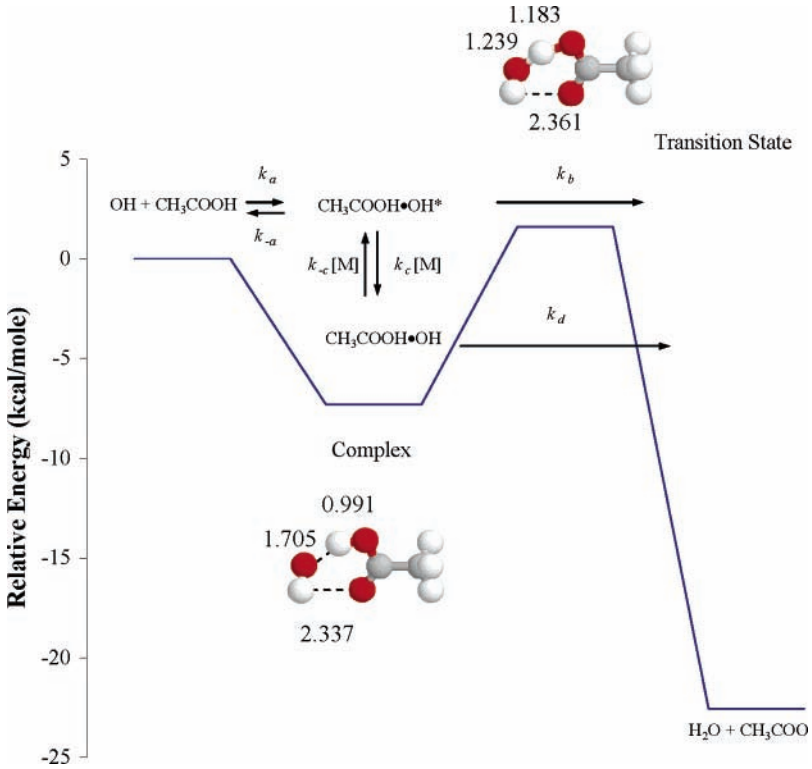

Figure 5. Schematic mechanism for the acidic hydrogen abstraction channel for the OH + acetic acid reaction with the individual rate constants indicated (see text). Zero-point corrected relative energies and structures are the calculated G2M//B3LYP/6-311++G(2df,2pd) energies of De Smedt et al.[50] Indicated bond lengths are in angstroms.

for the OH + formic acid reaction, where abstraction of the acidic hydrogen is the primary pathway for the reaction.[52−54] The negative temperature dependence for the OH + acetic acid reaction observed in this study and by Singleton et al.[34] and Butkovskaya et al.[30] is consistent with this mechanism,[30,49,52,55] and the agreement between the low-pressure measurements reported here with the previous measurements at higher pressures suggests that the binding energy of the complex is small, resulting in rates of stabilization that are independent of pressure.

The relatively large primary kinetic isotope effect (KIE) for this reaction suggests that quantum mechanical tunneling may be important in the reaction mechanism. The primary KIE ($k_{\text{acetic acid}}/k_{\text{acetic acid}-d_4}$) in our low-pressure experiments varied from a high of 7.0 at 330 K to a low of 4.8 at 273 K with a value of (6.8 ± 0.21) at 300 K. This is larger than the KIE observed by Singleton et al., which varied between 4.3 at 356 K and 3.5 at 446 K with a value of (3.67 ± 0.14) at 297 K.[34] However, the observed KIE in our study is similar to that observed for the OH + acetone reaction, which also likely proceeds by hydrogen abstraction via a hydrogen-bonded complex.[39,49]

To determine whether the observed kinetic isotope effect for the OH + acetic acid reaction is consistent with the acidic hydrogen abstraction mechanism involving an intermediate complex, ab initio calculated energies, structures and frequencies of the intermediate complexes and transition states for the OH + acetic acid reaction were used in conjunction with RRKM theory to calculate the kinetic isotope effect for this reaction as a function of temperature. A schematic for the potential energy surface for abstraction of the acidic hydrogen is shown in Figure 5 and is similar to the mechanism proposed for the OH + HNO_3 and OH + acetone reactions.[49] The first step in the mechanism involves the formation of an excited OH−acetic acid complex (k_a), which can dissociate to re-form the reactants (k_{-a}), react to lead to product formation (k_b), or be collisionally stabilized to form the thermalized OH− acetic acid complex (k_c[M]). The thermalized complex can be collisionally activated to form the excited complex (k_{-c}[M]), or react to form products (k_d). The influence of quantum mechanical tunneling on k_b and k_d may enhance the kinetic isotope effect for this reaction.

The detailed ab initio study of this channel by De Smedt et al. found several hydrogen-bonded pre-reactive complexes with stabilization energies ranging from 3.1 to 7.3 kcal/mol at the G2M(CC,MP2)//B3LYP/6-311++G(2df,2pd) level of theory.[50] The most stable complex involves a six-member hydrogen-bonded ring similar to the structure found by Rosado-Reyes and Francisco at the QCISD/6-31G(d) level of theory (Figure 5).[51] These pre-reactive complexes are expected to interconvert easily and reach a rapid equilibrium as the barriers for rearrangement are relatively low and lie below the energy of the reactants.[50] For simplicity, only the hydrogen-bonded ring complex was considered in these calculations, as it is the most stable pre-reactive complex and will contribute the most to the thermal equilibrium population.[50]

The relative energies of the pre-reactive complex and transition state for both the OH + acetic acid and OH + acetic acid-d_4 reactions used in the RRKM calculations are shown in Table 2 and reflect the G2M(CC,MP2) calculated energies reported by De Smedt et al., corrected for the unscaled zero point energy at the B3LYP/6-311++G(2df,2pd) optimized geometry.[50] De Smedt et al. found that the calculated energies of the transition states at the highest levels of theory agreed to within a few tenths of a kilocalorie per mole, except for the energy of the critical transition state for acidic hydrogen abstraction, where the energy differences at the highest levels of theory varied from a value of 1.6 kcal/mol at the G2M(CC,MP2)//B3LYP/6-311++G(2df,2pd) level of theory, to 5.3 kcal/mol using G3 theory, with the G2M(CC,MP2) barrier heights leading to calculated absolute rate constants that were in better agreement with experiment.[50] For simplicity, the G2M(CC,MP2)// B3LYP/

TABLE 2: Calculated Frequencies and Energies Relative to Reactants Used in the RRKM Calculations for the OH + Acetic Acid Reaction

species	B3LYP/6-311++G(2df,2pd) frequencies (cm^{-1})	zero point energy (kcal mol^{-1})	G2M relative energies[a] (kcal mol^{-1})
OH	3714	5.3	
acetic acid	3757, 3165, 3113, 3056, 1816, 1479, 1473, 1408, 1336, 1202, 1070, 999, 859, 664, 585, 547, 425, 76	38.6	
OH−acetic acid complex	3775, 3229, 3166, 3117, 3058, 1720, 1479, 1469, 1414, 1383, 1309, 1072, 1028, 955, 892, 621, 604, 483, 435, 320, 223, 189, 111, 72	45.9	−7.3
OH−acetic acid TS	3800, 3162, 3123, 3059, 1711, 1653, 1480, 1470, 1453, 1406, 1389, 1067, 1035, 941, 745, 667, 601, 556, 457, 403, 264, 141, 68, 1306*i*	43.8	1.6
acetic acid-d_4	2733, 2347, 2303, 2196, 1804, 1293, 1093, 1066, 1052, 1018, 933, 824, 754, 548, 535, 418, 373, 55	30.5	
OH−acetic acid-d_4 complex	3775, 2352, 2348, 2306, 2197, 1688, 1349, 1111, 1080, 1066, 1051, 938, 837, 794, 708, 578, 520, 473, 388, 317, 216, 185, 103, 53	37.8	−7.3
OH-acetic acid-d_4 TS	3800, 2346, 2311, 2196, 1598, 1440, 1223, 1112, 1103, 1065, 1049, 930, 893, 839, 710, 628, 533, 525, 451, 372, 253, 133, 50, 967*i*	36.5	2.5

[a] Based on the unscaled zero point corrected G2M(CC,MP2)//B3LYP/6-311++G(2df,2pd) energies of De Smedt et al.[50] for the OH + acetic acid reaction.

TABLE 3: Calculated Rate Coefficients for the Individual Reactions in the Acidic Hydrogen Abstraction Mechanism for the OH + Acetic Acid and OH + Acetic Acid-d_4 Reactions

temp (K)	$10^{-5}K_{eq}$	$10^{-8}k_{-a}$ (s^{-1})	$10^{-6}k_b$ (s^{-1})	$10^{-2}k_d$ (s^{-1})	$10^{13}k$ (calc) (cm^3 s^{-1})
		OH + acetic acid			
400	0.05	51.3	30.5	97.3	4.2
340	0.1	10.5	11.4	7.7	5.0
300	0.3	2.5	4.2	0.8	6.6
240	2.5	0.1	0.6	0.001	14.6
220	7.4	0.03	0.2	0.0002	22.6
200	29.4	0.005	0.08	1×10^{-5}	40.0
		OH + acetic acid-d_4			
400	0.006	56.4	8.8	16.8	0.46
340	0.01	11.5	3.3	0.9	0.78
300	0.03	2.7	1.2	0.06	1.2
240	0.2	0.1	0.2	2×10^{-5}	3.9
220	0.7	0.03	0.07	3×10^{-6}	6.0
200	2.5	0.005	0.02	8×10^{-8}	11.5

6-311++G(2df,2pd) calculated energies of De Smedt et al. were used in these calculations (Table 2). These relative energies are similar to those calculated by Rosado-Reyes and Francisco at the QCISD(T)/6-31++G(2df,2p) level of theory, who found a binding energy for the pre-reactive complex of 6.5 kcal/mol, and a barrier height for subsequent reaction of 2.1 kcal/mol relative to the reactants.[51] This small stabilization energy for the pre-reactive complex is consistent with the observed lack of a pressure dependence of the rate constant for this reaction. For the OH + acetic acid-d_4 reaction, the G2M(CC,MP2) energies of De Smedt et al.[50] were corrected by the unscaled ZPE energy differences between the OH + acetic acid system and the deuterated system. The frequencies of the pre-reactive complex and the transition state for the OH + acetic acid-d_4 reaction system were calculated at the B3LYP/6-311++G(2df,-2pd) level of theory using the Gaussian 03 system of programs[56] based on the B3LYP/6-311++G(2df,2pd) optimized geometries of De Smedt et al.,[50] and are shown in Table 2 with the OH + acetic acid frequencies for comparison.

Based on the mechanism shown in Figure 5 and assuming that the intermediate complex is in steady-state, the overall rate constant for the OH + acetic acid reaction can be expressed by[57]

$$k = k_a\left(\frac{k_a + K_{eq}k_d}{k_{-a} + k_b + K_{eq}k_d}\right) \qquad (7)$$

In this equation, K_{eq} is the equilibrium constant between the excited and stabilized complex (k_c/k_{-c}). Assuming that the rate constants for formation of the activated complex for the OH + acetic acid and acetic acid-d_4 reactions are similar to that for the OH + acetone reaction and are independent of temperature (2.67 and 3.45 × 10^{-11} cm^3 $molecule^{-1}$ s^{-1}, respectively),[57] k_{-a} can be estimated as a function of temperature from the temperature-dependent equilibrium constant for complex formation determined by the stabilization energy and the partition functions for the complex and reactants ($K_f = Q_{complex}/(Q_{OH}Q_{Acetic\ acid}\exp(-\Delta E/RT))$. Using the ab initio stabilization energy and frequencies shown in Table 2, the calculated values for the equilibrium constant for complex formation varied from 6 × 10^{-17} cm^3 $molecule^{-1}$ at 200 K to 6 × 10^{-21} cm^3 $molecule^{-1}$ at 400 K.

The value of K_{eq}, the equilibrium constant between the excited and stabilized complex (k_c/k_{-c}), can be estimated as a function of temperature using RRKM theory:[58]

$$K_{eq} = \frac{k_c}{k_{-c}} = \frac{Q_c}{P(E^*)\exp(-E^*/kT)} \qquad (8)$$

In this equation, Q_c is the partition function for the active modes of the complex, and $P(E^*)$ is the number of quantum states near the dissociation threshold E* determined using a Beyer−Swinehart counting algorithm. For simplicity, only vibrational modes were used in the calculation.

Table 3 shows the estimated values of K_{eq}, and k_{-a} calculated at several temperatures for the OH + acetic acid and OH + acetic acid-d_4 reactions. Similar to previous calculations for the OH + acetone reaction,[39,57] values of k_b and k_d for the OH + acetic acid reaction were determined from a fit of eq 7 using the calculated values of K_{eq} and k_{-a} to the three-parameter expression for the overall rate constant of Butkovskaya et al.[30] Values of k_b and k_d for the OH + acetic acid-d_4 reaction were then determined from the corresponding values for the OH + acetic acid reaction by calculating the kinetic isotope effect for these unimolecular dissociation rate constants.

The kinetic isotope effect for the rate constant for the formation of products from the energized complex (k_b) was estimated using the following expression from RRKM theory:[58]

$$\frac{k_{bH}(E^*_H)}{k_{bD}(E^*_D)} = \frac{W_H(E^+)/\rho_H(E^*_H)}{W_D(E^+)/\rho_D(E^*_D)} \qquad (9)$$

In this equation, $W(E^+)$ is the sum of quantum states in the transition state and $\rho(E^*)$ is the density of states of the excited complex for the OH−acetic acid and OH−acetic acid-d_4 reactions. Given the uncertainty associated with the barrier height for the transition state leading to the formation of products, tunneling corrections were not included. Considering only the vibrational modes for simplicity and using the ab initio calculated frequencies for the complex and the transition state, this equation leads to an estimated kinetic isotope effect for k_b of approximately 3.5.

The kinetic isotope effect for the rate constant for the formation of products from the stabilized complex (k_d) was estimated using the RRKM expression for the high-pressure limiting rate constants:[58]

$$\frac{k_{d_H}}{k_{d_D}} = \frac{\Gamma_H}{\Gamma_D}\frac{(Q^+/Q)_H}{(Q^+/Q)_D}\exp\{[(E_0)_D - (E_0)_H]/kT\} \qquad (10)$$

In this equation, Q^+ and Q are the partition functions for the active degrees of freedom in the transition state and the stabilized complex, respectively, E_0 is the zero-point corrected barrier height for the transition state relative to the complex, and Γ_H and Γ_D are the tunneling transmission coefficients for the acetic acid and acetic acid-d_4 systems, respectively. The tunneling coefficients were estimated for transmission through an asymmetric one-dimensional Eckart potential using the ab initio calculated barrier heights and exothermicities of the complexes relative to the transition state and products, and the calculated imaginary frequencies for the OH−acetic acid and OH−acetic acid-d_4 acidic hydrogen abstraction transition states at the B3LYP/6-311++G(2df,2pd) level of theory (1306i and 967i, respectively).[59] The calculated kinetic isotope effect for k_d from this equation varied from approximately 5.8 at 400 K to 150 at 200 K.

The calculated k_b, k_d and overall rate constants for the OH + acetic acid-d_4 reaction are shown in Table 3, and the calculated overall rate constants from eq 7 are also plotted in Figure 3 for both the OH + acetic acid (upper solid line) and the OH + acetic acid-d_4 reactions (lower solid line). As can be seen from this figure, the calculated rate constants as a function of temperature for the OH + acetic acid-d_4 reaction are in good agreement with the rate constants measured in this study, with the predicted rate constants falling between the results of this study and the results of Singleton et al.[34] This suggests that the large kinetic isotope effect observed in these studies is consistent with a mechanism involving abstraction of the acidic hydrogen through the formation of an intermediate complex.

In contrast to the OH + acetone reaction, where similar calculations suggest that the reaction of the stabilized complex contributes significantly to the overall rate constant below room temperature,[39,57] the results of this simple model of the OH + acetic acid reaction suggest that reactions of the excited complex dominate the overall rate constant for this reaction below room temperature, as the product of $K_{eq}k_d$ is significantly smaller than k_b and k_{-a} for this temperature range. This is not surprising, as the barrier for the reaction of the stabilized complex for the OH + acetic acid reaction is higher (approximately 9 kcal/mol) than that for the OH + acetone reaction (approximately 3.5 kcal/mol). On the basis of these simple calculations, reactions of the excited complex dominate the mechanism at low temperatures and reactions of the stabilized complex become more important to the overall mechanism at higher temperatures. The agreement of the low pressure measurements of the rate constant as a function of temperature with those measured at higher pressures suggest that the rate of stabilization of the excited complex is independent of pressure for the conditions of these experiments. However, additional measurements at low pressure are needed, especially at temperatures below 260 K to confirm that reactions of the excited complex are not enhanced at low temperatures and low pressure compared to atmospheric pressure.

Because the results of this simple model of the OH + acetic acid reaction suggest that reactions of the excited complex dominate the overall rate constant for this reaction below room temperature, the calculated KIE for the OH + acetic acid reaction at lower temperatures is primarily due to the KIE of the rate constants for the reactions of the excited complex. As the temperature increases, the rate of reaction of the stabilized complex increases such that the product of $K_{eq}k_d$ becomes significant relative to k_b, and the calculated KIE increases as quantum mechanical tunneling enhances k_d for the OH + acetic acid reaction relative to the OH + acetic acid-d_4 reaction. Because tunneling was not included in the calculations of the rate constant for the reaction of the excited complex (k_b), these calculations may underestimate the overall kinetic isotope effect and the contribution of quantum mechanical tunneling to this reaction.

These simple calculations do not take into account the contribution of hydrogen abstraction from the methyl group to the overall rate constant. Theoretical calculations suggest that although this pathway likely proceeds through a hydrogen-bonded pre-reactive complex, the barrier for hydrogen abstraction from the methyl group is higher than abstraction of the acidic hydrogen.[50,51] As a result, the branching ratio for methyl hydrogen abstraction is expected to increase with temperature[50] and may contribute to the curvature in the Arrhenius plots observed by Singleton et al.[34]

Conclusions

Measurements of the kinetics of the OH + acetic acid reactions using discharge-flow techniques at 2−5 Torr and between 263 and 373 K are in excellent agreement with the results of Butkovskaya et al.[30] below room temperature as well as those of Singleton et al.[34] above room temperature but are in contrast to the reported positive temperature dependence of Dagaut et al.[33] These results are also in good agreement with the recent recommendation of Atkinson et al. for the temperature dependence of this reaction[60] but suggest that the current recommendation of Sander et al.[35] with a weak negative temperature dependence may overestimate the chemical lifetime of acetic acid in the atmosphere and underestimate the contribution of acetic acid to the oxidation capacity of the upper troposphere.[30]

Measurements of the rate constants for the OH + acetic acid-d_3 and OH + acetic acid-d_4 reactions suggest that the primary mechanism for this reaction involves abstraction of the acidic hydrogen, consistent with recent measurements of the CO_2 yield of this reaction.[30,50] RRKM calculations of the kinetic isotope effect for the reaction as a function of temperature based on the ab initio calculated energies and frequencies[50] are consistent with a mechanism involving abstraction of the acidic hydrogen through a hydrogen bonded intermediate complex. However, additional experimental measurements and more detailed theoretical calculations are needed to confirm these results.

Acknowledgment. This work was supported by the National Science Foundation (grant ATM-9984152), and in part by Shared University Research grants from IBM, Inc. to Indiana University.

References and Notes

(1) Kawamura, K.; Steinberg, S.; Kaplan, I. R. *Atmos. Environ.* **1996**, *30*, 1035.

(2) Pio, C.; Alves, C.; Duarte, A. *Atmos. Environ.* **2001**, *35*, 389.

(3) Fraser, M. P.; Cass, G. R.; Simoneit, B. R. T. *Environ. Sci. Technol.* **2003**, *37*, 446.

(4) Keene, W. C.; Galloway, J. N. *J. Geophys. Res.* **1986**, *91*, 14466.

(5) Galloway, J. N.; Keene, W. C.; Likens, G. E. *J. Geophys. Res.* **1996**, *101*, 6883.

(6) Khare, P.; Kumar, N.; Kumari, K. M.; Srivastava, S. S. *Rev. Geophys.* **1999**, *37*, 227.

(7) Alfonso, L.; Raga, G. B. *Atmos. Chem. Phys.* **2004**, *4*, 1097.

(8) Monod, A.; Carlier, P. *Atmos. Environ.* **1999**, *33*, 4431.

(9) Talbot, R. W.; Beecher, K. M.; Harriss, R. C.; Cofer, W. R. *J. Geophys. Res.* **1988**, *93*, 1638.

(10) Hartmann, W. R.; Santana, M.; Hermoso, M.; Andreae, M. O.; Sanhueza, E. *J. Atmos. Chem.* **1991**, *13*, 63.

(11) Kesselmeier, J.; Staudt, M. *J. Atmos. Chem.* **1999**, *33*, 23.

(12) Grosjean, D. *Environ. Sci. Technol.* **1989**, *23*, 1506.

(13) Kawamura, K.; Ng, L. L.; Kaplan, I. R. *Environ. Sci. Technol.* **1985**, *19*, 1082.

(14) Kawamura, K.; Steinberg, S.; Kaplan, I. R. *Atmos. Environ.* **2000**, *34*, 4175.

(15) Zervas, E.; Tazerout, M. *Atmos. Environ.* **2000**, *34*, 3921.

(16) Zervas, E.; Montagne, X.; Lahaye, J. *Environ. Sci. Technol.* **2002**, *36*, 2414.

(17) Sanhueza, E.; Figueroa, L.; Santana, M. *Atmos. Environ.* **1996**, *30*, 1861.

(18) Talbot, R. W.; Andreae, M. O.; Berresheim, H.; Jacob, D. J.; Beecher, K. M. *J. Geophys. Res.* **1990**, *95*, 16799.

(19) Atkinson, R. *Atmos. Environ.* **1990**, *24*, 1.

(20) Singh, H. B.; Ohara, D.; Herlth, D.; Sachse, W.; Blake, D. R.; Bradshaw, J. D.; Kanakidou, M.; Crutzen, P. J. *J. Geophys. Res.* **1994**, *99*, 1805.

(21) Horie, O.; Moortgat, G. K. *J. Chem. Soc., Faraday Trans.* **1992**, *88*, 3305.

(22) Horie, O.; Moortgat, G. K. *Acc. Chem. Res.* **1998**, *31*, 387.

(23) Madronich, S.; Chatfield, R. B.; Calvert, J. G.; Moortgat, G. K.; Veyret, B.; Lesclaux, R. *Geophys. Res. Lett.* **1990**, *17*, 2361.

(24) Lawrence, J.; Koutrakis, P. *J. Geophys. Res.* **1996**, *101*, 9171.

(25) Tyndall, G. S.; Cox, R. A.; Granier, C.; Lesclaux, R.; Moortgat, G. K.; Pilling, M. J.; Ravishankara, A. R.; Wallington, T. J. *J. Geophys. Res.* **2001**, *106*, 12157.

(26) Baboukas, E. D.; Kanakidou, M.; Mihalopoulos, N. *J. Geophys. Res.* **2000**, *105*, 14459.

(27) Jacob, D. J.; Heikes, B. G.; Fan, S. M.; Logan, J. A.; Mauzerall, D. L.; Bradshaw, J. D.; Singh, H. B.; Gregory, G. L.; Talbot, R. W.; Blake, D. R.; Sachse, G. W. *J. Geophys. Res.* **1996**, *101*, 24235.

(28) Jacob, D. J.; Wofsy, S. C.; Bakwin, P. S.; Fan, S. M.; Harriss, R. C.; Talbot, R. W.; Bradshaw, J. D.; Sandholm, S. T.; Singh, H. B.; Browell, E. V.; Gregory, G. L.; Sachse, G. W.; Shipham, M. C.; Blake, D. R.; Fitzjarrald, D. R. *J. Geophys. Res.* **1992**, *97*, 16421.

(29) Chebbi, A.; Carlier, P. *Atmos. Environ.* **1996**, *30*, 4233.

(30) Butkovskaya, N. I.; Kukui, A.; Pouvesle, N.; Le Bras, G. *J. Phys. Chem. A* **2004**, *108*, 7021.

(31) Reiner, T.; Mohler, O.; Arnold, F. *J. Geophys. Res.* **1999**, *104*, 13943.

(32) Zetzsch, C.; Stuhl, F. In *Physico-Chemical Behaviour of Atmospheric Pollutants;* Versino, B., Ott, H., Eds.; Vol. Proceedings of the Second European Symposium; D. Reidel: Dordrecht, The Netherlands, 1982; p 129.

(33) Dagaut, P.; Wallington, T. J.; Liu, R. Z.; Kurylo, M. J. *Int. J. Chem. Kinet.* **1988**, *20*, 331.

(34) Singleton, D. L.; Paraskevopoulos, G.; Irwin, R. S. *J. Am. Chem. Soc.* **1989**, *111*, 5248.

(35) Sander, S. P.; Friedl, R. R.; Golden, D. M.; Kurylo, M. J.; Huie, R. E.; Orkin, V. L.; Moortgat, G. K.; Ravishankara, A., R.; Kolb, C. E.; Molina, M. J.; Finlayson-Pitts, B. J. *Chemical Kinetics and Photochemical Data for Use in Atmospheric Studies*; Evaluationn Number 14; Jet Propulsion Laboratory: Pasadena, CA, 2003.

(36) Stevens, P.; L'Esperance, D.; Chuong, B.; Martin, G. *Int. J. Chem. Kinet.* **1999**, *31*, 637.

(37) Chuong, B.; Stevens, P. S. *J. Phys. Chem. A* **2000**, *104*, 5230.

(38) Chuong, B.; Stevens, P. S. *J. Phys. Chem. A* **2003**, *107*, 2185.

(39) Davis, M. E.; Drake, W.; Vimal, D.; Stevens, P. S. *J. Photochem. Photobiol. A* **2005**, *176*, 162.

(40) Bedjanian, Y.; Laverdet, G.; Le Bras, G. *J. Phys. Chem. A* **1998**, *102*, 953.

(41) Stutz, J.; Ezell, M. J.; Ezell, A. A.; Finlayson-Pitts, B. J. *J. Phys. Chem. A* **1998**, *102*, 8510.

(42) Chuong, B.; Davis, M.; Edwards, M.; Stevens, P. S. *Int. J. Chem. Kinet.* **2002**, *34*, 300.

(43) Davis, M. E.; Stevens, P. S. *Atmos. Environ.* **2005**, *39*, 1765.

(44) Chao, J.; Zwolinski, B. J. *J. Phys. Chem. Ref. Data* **1978**, *7*, 363.

(45) Crawford, M. A.; Wallington, T. J.; Szente, J. J.; Maricq, M. M.; Francisco, J. S. *J. Phys. Chem. A* **1999**, *103*, 365.

(46) Orlando, J. J.; Tyndall, G. S. *J. Photochem. Photobiol. A* **2003**, *157*, 161.

(47) Howard, C. J. *J. Phys. Chem.* **1979**, *83*, 3.

(48) Cvetanovic, R. J.; Singleton, D. L.; Paraskevopoulos, G. *J. Phys. Chem.* **1979**, *83*, 50.

(49) Smith, I. W. M.; Ravishankara, A. R. *J. Phys. Chem. A* **2002**, *106*, 4798.

(50) De Smedt, F.; Bui, X. V.; Nguyen, T. L.; Peeters, J.; Vereecken, L. *J. Phys. Chem. A* **2005**, *109*, 2401.

(51) Rosado-Reyes, C. M.; Francisco, J. S. *J. Phys. Chem. A* **2006**, *110*, 4419.

(52) Galano, A.; Alvarez-Idaboy, J. R.; Ruiz-Santoyo, M. E.; Vivier-Bunge, A. *J. Phys. Chem. A* **2002**, *106*, 9520.

(53) Anglada, J. M. *J. Am. Chem. Soc.* **2004**, *126*, 9809.

(54) Torrent-Sucarrat, M.; Anglada, J. M. *Chemphyschem* **2004**, *5*, 183.

(55) Aloisio, S.; Francisco, J. S. *Acc. Chem. Res.* **2000**, *33*, 825.

(56) Frisch, M. J.; Trucks, G. W.; Schlegel, H. B.; Scuseria, G. E.; Robb, M. A.; Cheeseman, J. R.; Montgomery, J. A., Jr.; Vreven, T.; Kudin, K. N.; Burant, J. C.; Millam, J. M.; Iyengar, S. S.; Tomasi, J.; Barone, V.; Mennucci, B.; Cossi, M.; Scalmani, G.; Rega, N.; Petersson, G. A.; Nakatsuji, H.; Hada, M.; Ehara, M.; Toyota, K.; Fukuda, R.; Hasegawa, J.; Ishida, M.; Nakajima, T.; Honda, Y.; Kitao, O.; Nakai, H.; Klene, M.; Li, X.; Knox, J. E.; Hratchian, H. P.; Cross, J. B.; Bakken, V.; Adamo, C.; Jaramillo, J.; Gomperts, R.; Stratmann, R. E.; Yazyev, O.; Austin, A. J.; Cammi, R.; Pomelli, C.; Ochterski, J. W.; Ayala, P. Y.; Morokuma, K.; Voth, G. A.; Salvador, P.; Dannenberg, J. J.; Zakrzewski, V. G.; Dapprich, S.; Daniels, A. D.; Strain, M. C.; Farkas, O.; Malick, D. K.; Rabuck, A. D.; Raghavachari, K.; Foresman, J. B.; Ortiz, J. V.; Cui, Q.; Baboul, A. G.; Clifford, S.; Cioslowski, J.; Stefanov, B. B.; Liu, G.; Liashenko, A.; Piskorz, P.; Komaromi, I.; Martin, R. L.; Fox, D. J.; Keith, T.; Al-Laham, M. A.; Peng, C. Y.; Nanayakkara, A.; Challacombe, M.; Gill, P. M. W.; Johnson, B.; Chen, W.; Wong, M. W.; Gonzalez, C.; Pople, J. A. *Gaussian 03*, revision B.05; Gaussian, Inc.: Wallingford, CT, 2004.

(57) Talukdar, R. K.; Gierczak, T.; McCabe, D. C.; Ravishankara, A. R. *J. Phys. Chem. A* **2003**, *107*, 5021.

(58) Holbrook, K. A.; Pilling, M. J.; Robertson, S. H. *Unimolecular Reactions*. 2md ed.; John Wiley and Sons: New York, 1996.

(59) Johnston, H. S.; Heicklen, J. *J. Phys. Chem.* **1962**, *66*, 532.

(60) Atkinson, R.; Baulch, D. L.; Cox, R. A.; Crowley, J. N.; Hampson, R. F.; Hynes, R. G.; Jenkin, M. E.; Kerr, J. A.; Rossi, M. J.; Troe, J. *IUPAC Subcommittee for Gas Kinetic Data Evaluation*, 2005, http://www.iupac-kinetic.ch.cam.ac.uk/index.html.